

# Esterification of Acetic Acid with Butanol in the Presence of Ion-Exchange Resins as Catalysts

Jignesh Gangadwala, Surendra Mankar, and Sanjay Mahajani\*

Department of Chemical Engineering, Indian Institute of Technology—Bombay, Powai, Mumbai 400076, India

Achim Kienle and Erik Stein

Max Plank Institute for Dynamics of Complex Technical Systems, Magdeburg 39106, Germany

The esterification of acetic acid with *n*-butanol was studied in the presence of ion-exchange resin catalysts such as Amberlyst-15 to determine the intrinsic reaction kinetics. The effect of various parameters such as temperature, mole ratio, catalyst loading, and particle size was studied. Kinetic modeling was performed to obtain the parameters related to intrinsic kinetics. Pseudohomogeneous, Eley–Rideal, Langmuir–Hinshelwood–Hougen–Watson (LHHW), and modified LHHW models were developed. The kinetics for the side-reaction etherification was also investigated. The rate expressions would be useful in the simulation studies for reactive distillation. The experimental data generated for the reaction under total reflux were validated successfully using the developed rate equation and estimated values of kinetic parameters.

## Introduction

Butyl acetate is an industrially important chemical with applications as a versatile solvent and an intermediate in organic synthesis. It is used in large quantities as a solvent for plastics, liquors, resins, gums, and coatings. It is its low volatility that makes it suitable for adjustment of the evaporation rate and viscosity. It may also be used in the photographic industry, as a reaction medium for adhesives, a solvent for leather dressings, an extraction solvent, and a process solvent in various industrial applications.

Butyl acetate is commonly synthesized through esterification of acetic acid with *n*-butanol in the presence of a suitable acid catalyst. This reaction is reversible, and the simultaneous removal of product(s) during the course of the reaction is beneficial in view of obtaining enhanced conversion. Various methods to remove product(s) have been adopted in the past, and the next section gives a summary of the same. The basic knowledge of intrinsic kinetics is of utmost importance in the design of the suitable commercial reactors for this reaction. Though reaction kinetics with various homogeneous catalysts is available, the rate expression for commonly used ion-exchange resins over a wide range of operating parameters is not evident in the open literature. This work is, therefore, mainly directed toward obtaining a suitable rate equation and checking its validity under different conditions.

## Previous Studies

The synthesis of butyl acetate through esterification has been carried out for several years now. One of the earliest systematic studies is by Othmer and co-workers, who investigated this reaction in the presence of sulfuric acid as a catalyst.<sup>1</sup> In recent years, the solid heterogeneous catalysts are receiving attention because of their

obvious engineering benefits such as ease of separation and fewer disposal and corrosion problems. Cation-exchange resin is considered to be an important catalyst for liquid-phase reactions like esterification, etherification, etc.<sup>2</sup> Zheng and Zeng have studied the kinetics of esterification in the presence of a strong cation-exchange resin.<sup>3,4</sup> They have investigated the influence of various parameters and proposed the rate equation. Liao and co-workers have also studied this reaction in the presence of solid acid cation-exchange resins.<sup>5–7</sup> There are a few other investigations on the reaction kinetics in the presence of various zeolitic catalysts.<sup>8–11</sup> Li et al. have studied various zeolites, such as HX, HY, HM, and HZSM5, for esterification of butanol with acetic acid and found that HZSM5 acts as the best catalyst from all zeolites studied.<sup>12</sup> Janowsky et al. have studied the kinetics in the presence of Lewatit SPC 108 and 118 catalysts and proposed a pseudohomogeneous (PH) kinetic model for the esterification reaction.<sup>13</sup> The expression for equilibrium constant (equation 1) proposed by them will be used in this work.

$$K_a = 3.8207 \exp(3.5817 \times 10^3/RT) \quad (1)$$

Several attempts have been made to improve the performance of the reaction. As mentioned earlier, different strategies for the simultaneous removal of product(s) during the course of the reaction have been attempted in the past. Reactive distillation has been one of such important means to achieve this objective. Both reaction and distillation are performed in a single piece of equipment to enhance the overall performance. It not only reduces the capital cost but also renders savings in view of energy and raw material consumption. Othmer's study is considered to be a classic example in this respect, and several other attempts have been made thereafter to investigate this reaction with reactive distillation either in a batch mode<sup>14</sup> or in a continuous mode.<sup>13,15,16</sup> One interesting finding of the experimental work by Janowsky et al.<sup>13</sup> on reactive distillation was the formation of the side product di-*n*-butyl ether (DBE) in the bottoms. The present work takes into account this

\* To whom correspondence should be addressed. Tel.: +91-22-5727246. Fax: +91-22-5726895. E-mail: sanjaym@che.iitb.ac.in.

important consideration and determines the conditions under which ether formation is significant.

The reaction can be an important tool for recovery of dilute acetic acid aqueous streams. Acetic acid from the aqueous solutions can be made to react with butanol to obtain butyl acetate, which can be directly sold or hydrolyzed back to acetic acid. Reactive distillation for recovery of the acetic acid stream typically in the form of 20–30% solution through this reaction has been investigated, and the extent of recovery is on the order of 40–50%.<sup>17</sup>

Another approach to increase the overall conversion is through the simultaneous extraction of butyl acetate. The reaction is performed in the presence of a strong acid such as sulfuric acid at relatively low temperatures.<sup>18</sup> However, ion-exchange resins are not active enough to catalyze the reaction at such low temperatures and may not be the suitable catalyst. At relatively high temperatures, phase splitting, which is essential for extractive reaction, does not occur unless one uses an external solvent.

Despite several such studies on this useful reaction, the basic investigation on intrinsic reaction kinetics in the presence of an emerging heterogeneous catalyst is quite limited. There has been no mention of the side reaction of ether formation in any of these studies. Hence, we believe that there is a need to develop a reliable rate equation, which is applicable over a wide range of operating parameters and can be conveniently used for the design of the reactor of interest, especially the reactive distillation column. It is with this intention that the present work has been undertaken.

## Experimental Section

**Materials and Catalysts.** *n*-Butanol and acetic acid (both AR grade) were obtained from s.d. Fine Chemicals Ltd., Thane, India. The catalyst Amberlyst-15 was obtained from Rohm and Haas: Philadelphia, PA. The catalysts TX-66 and Inidon-130 were supplied by Thermax India Ltd., Pune and Ion exchange India Ltd., Mumbai, respectively. The catalysts in the supplied form were reasonably dry. They were dried further for 6 h in a vacuum. However, it was observed that the catalyst activity toward esterification remains unchanged with and without drying. This may be because of the formation and the presence of water in the reaction mixture. However, it was observed through separate studies on the etherification reaction that the drying of catalyst makes a significant improvement in the reaction rate. Hence, all etherification runs were conducted with a catalyst dried using the above procedure.

**Apparatus and Procedure.** The esterification reaction was performed in a  $3 \times 10^{-4}$  m<sup>3</sup> glass reactor dipped in the constant-temperature oil bath. The reactor was equipped with the temperature and speed monitoring facility. The measured quantities of *n*-butanol and acetic acid were charged to the reactor, and the reactor was dipped in the oil bath. Once the desired reaction temperature was attained, the catalyst was charged to the reactor, and this time was considered the zero reaction time. The samples were withdrawn after specific time intervals. Because the withdrawn samples contain no catalyst, no further reactions can take place in the samples even at high temperatures. However, to prevent evaporation losses, the samples were stored in

a refrigerator at around 278 K. The samples were then analyzed using the method described in the next section.

Because etherification reactions were performed at slightly higher temperatures than the boiling point of the reaction temperatures, a stainless steel autoclave of  $1.5 \times 10^{-4}$  m<sup>3</sup> capacity equipped with the temperature and speed control facility was used for this purpose. The catalyst and *n*-butanol were added to the reactor, and heating was started with slow stirring. Once the desired temperature was attained, the speed of agitation was increased, and this time was considered the zero reaction time.

To validate the model and its parameters, a separate set of experimental runs under different conditions were performed. The reaction was performed under boiling conditions under total reflux. The change in composition and temperature with respect to time was noted down.

**Analysis.** Both titration and gas chromatography were used for the analysis of the reaction mixture. The titration was performed using 0.5 N sodium hydroxide in the presence of a phenolphthalein indicator. The reliability of the titration method was confirmed with the help of analysis of standard samples containing butyl acetate to ensure that the hydrolysis of ester does not take place during the course of titration.

The individual products were analyzed using a gas chromatograph (C-911; Mak Analytica, India Ltd.) equipped with a thermal conductivity detector. The column used for analysis was Porapack-Q with hydrogen as a carrier gas at a flow rate of  $5 \times 10^{-7}$  m<sup>3</sup>/s. The injector and detector were maintained at temperatures of 493 and 423 K, respectively. The oven temperature was suitably programmed to get the best resolution and the least time for analysis. The initial oven temperature was 483 K, which was then increased further with a ramp rate of 20 K/min to 513 K and maintained there for 2 min. The retention times of all of the individual compounds were verified using authentic samples. Only DBE forms as a side product in this reaction. However, it was found that its formation is possible only under harsh conditions such as large catalyst loading, high temperature, and large *n*-butanol/acetic acid mole ratios. Hence, unless otherwise mentioned, all of the kinetic runs reported here are associated with negligible formation of the ether.

For the separate studies on the etherification reaction, the analysis was performed on the same gas chromatograph but with the help of a relatively polar SE-30 column at 363 K constant oven temperature under otherwise similar conditions.

## Elimination of Mass-Transfer Resistance

In this reaction, there exist two types of mass-transfer resistances, one across the solid–liquid interface and the other in the intraparticle space. The effect of the speed of agitation was studied over a wide range of 150–1300 rpm to examine the influence of an external mass-transfer effect. Figure 1 shows the results obtained. It is clear from the figure that the external mass-transfer resistance is negligible above 1000 rpm. Hence, all of the experiments were performed at this speed of agitation.

The possible influence of an internal mass transfer may be studied with different particle sizes. Figure 2 shows the effect of the average particle size on the reaction kinetics. The resin particles of the available size were ground to obtain finer particles. It can be seen that,

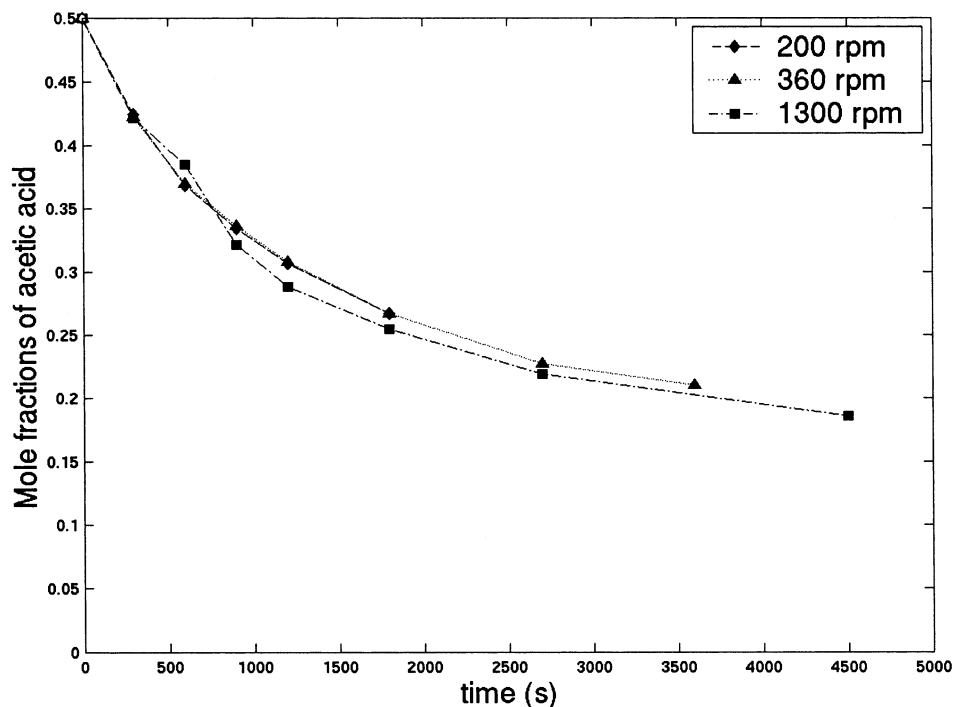


**Figure 1.** Effect of the speed of agitation (rpm) on the acetic acid mole fraction.  $T = 356$  K,  $M_{\text{cat}} = 6.67$  g of catalyst/gmol of AcH, and mole ratio of AcH:BuOH = 1:1.

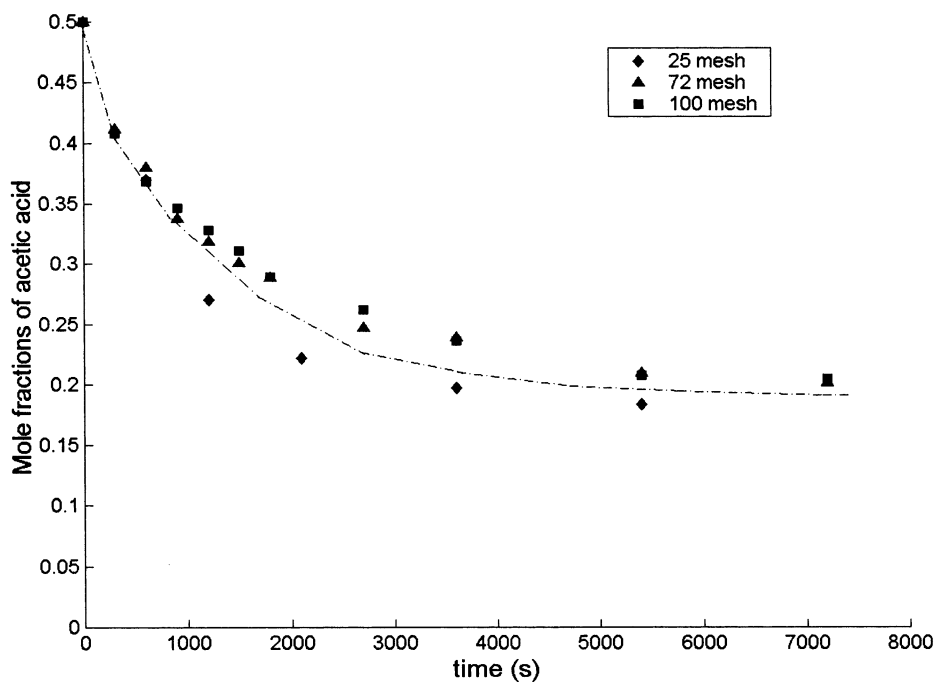


**Figure 2.** Effect of the catalyst particle size on the acetic acid mole fraction.  $T = 356$  K,  $M_{\text{cat}} = 6.67$  g of catalyst/gmol of AcH, and mole ratio of AcH:BuOH = 1:1.

over a wide range of particle sizes, the reaction rate hardly gets influenced. This indicates that the resistance due to intraparticle diffusion is insignificant. Hence, the resin was used in the supplied form for all of the kinetic runs.

#### Reaction with Other Ion-Exchange Resins

The reaction was studied with the other ion-exchange resins such as gel-type resin Amberlite IR-120 and the macroporous counterparts of Amberlyst-15, viz., Indion-130 and TX-66. The properties of all of the resins used are listed in Table 1.

It was observed that, among the macroporous resins, Amberlyst-15 gives the best performance, whereas activities for both gel-type Amberlite IR-120 and macroporous Amberlyst-15 were found to be similar for this reaction (Figure 3). The reaction mixture contains a substantial amount of water, which is responsible for the desired swelling of gel-type Amberlite IR-120, which in turn offers an activity equivalent to that of Amberlyst-15.

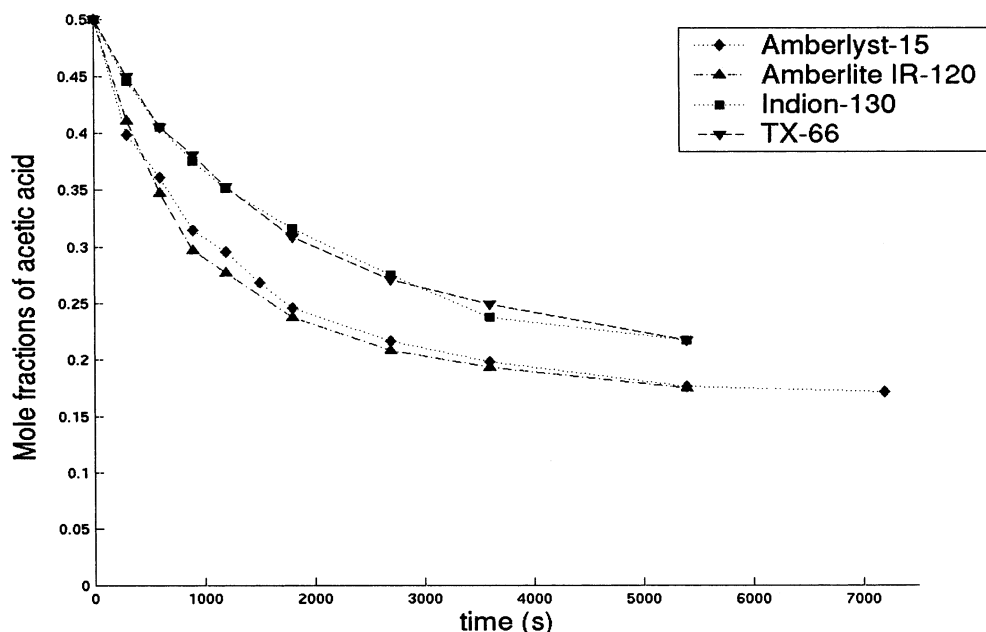
#### Development of a Kinetic Model

Because all of the experiments were conducted in the presence of a solid ion-exchange resin catalyst, hetero-

**Table 1. Physical Properties of the Ion-Exchange Resins Used in the Present Work**

properties	Amberlyst-15	Indion-130	Amberlite IR-120	Tulsion TX-66 MP
shape	beads	beads	beads	beads
average size (mm)	0.5	0.55	0.5	0.57
internal surface area (m <sup>2</sup> /g)	55	<i>a</i>	<i>a</i>	<i>a</i>
weight capacity (mequiv of W/g)	4.7	4.8	4.44	4.2
cross-linking density (% DVB)	20–25	<i>a</i>	8	<i>a</i>
porosity (%)	36	<i>a</i>	<i>b</i>	<i>a</i>
temperature stability (K)	393	403	393	393

<sup>a</sup> Data not available. <sup>b</sup> Data not applicable.

**Figure 3.** Effect of the catalyst type on the acetic acid mole fraction.

geneous kinetic models including PH, Eley–Rideal (RE), Langmuir–Hinshelwood–Hougen–Watson (LHHW), and modified LHHW (ML) were applied to correlate the kinetic data available for different temperatures, catalyst loadings, and mole ratios of acetic acid to butanol. In the preceding sections, it has been mentioned that the formation of DBE requires high temperatures and high catalyst loadings. In the temperature range studied for the esterification reaction of butanol with acetic acid, the formation of DBE was below the detection limit of the gas chromatograph instrument. Hence, the kinetic model for the esterification reaction was first developed using the data obtained over a temperature range of 333–363 K, a catalyst loading between 1 and 20 g of catalyst/gmol of acetic acid, and a mole ratio of 1:3 (acetic acid/butanol). To obtain kinetic parameters for the side reaction, separate experiments were performed at higher temperatures and higher catalyst loadings with pure *n*-butanol as the only feed to the reactor.

### Parameter Identification

The aim of the data-fitting procedure is to minimize the mean-square difference between calculated values of the mole fraction of acetic acid (or butanol for the side reaction) and that obtained through experiments. Mathematically, this can be expressed by eq 2. For the

$$\min_p \phi = \sum_{\text{all samples}} (x_{\text{AcH,cal}} - x_{\text{AcH,exp}})^2 \quad (2)$$

optimization procedure, the Sequential Quadratic Programming method from the NAG library<sup>19</sup> was used.

An SDASAC integrator was used to integrate the model equations.<sup>20</sup>

### PH Model for the Esterification Reaction

The PH model for the reaction rate can be written as

$$r_i = n \frac{dx_i}{dt} = \nu_i M_{\text{cat}} K_f \left( a_{\text{AcH}} a_{\text{BuOH}} - \frac{1}{K_a} a_{\text{BuAc}} a_{\text{H}_2\text{O}} \right) \quad (3)$$

where  $\nu_i$  is the stoichiometric coefficient of the  $i$ th component,  $M_{\text{cat}}$  is the catalyst mass,  $a_i (=x_i \gamma_i)$  is the activity of the  $i$ th component in the bulk liquid phase,  $x_i$  is mole fraction of the  $i$ th component, and  $\gamma_i$  is the activity coefficient of the  $i$ th component. The UNIQUAC model was used to determine the activity coefficients in the liquid phase. The binary coefficients and UNIQUAC equations are given in Table 2.  $K_f$  and  $K_a$  are the forward reaction rate constant and equilibrium constant, respectively. The temperature dependency of the rate constants  $K_i$  can be expressed by the Arrhenius equation

$$K_i = K_i^0 \exp(-E_i/RT) \quad (4)$$

Four adjustable parameters, namely, the preexponential factors  $K_f^0$  and  $K_a^0$  and the energies of activation  $E_f$  and  $E_a$ , have to be determined. As discussed before, the value of  $K_a$  is taken from Janowsky et al.<sup>13</sup> Hence, the number of parameters reduces to two. However, with only two free parameters, it was not possible to fit the data well, so preexponential factor  $K_a^0$  was also varied

**Table 2. UNIQUAC Activity Coefficient Model<sup>a</sup>**

volume parameters for the UNIQUAC equation		
component	<i>r</i>	<i>q</i>
acetic acid (1)	2.2024	2.072
butanol (2)	3.4543	3.052
butyl acetate (3)	4.8274	4.196
water (4)	0.9200	1.400
DBE	6.0925	5.176

**Model Equations**

$$\ln \gamma_i = \ln \gamma_i^C + \ln \gamma_i^R$$

$$\ln \gamma_i^C = \ln \varphi_i + I_i + \frac{z}{2} q_i \ln v_i - \varphi_i \sum_{j=1}^{nc} x_j J_j$$

$$\ln \gamma_i^R = q_i \left\{ 1 - \ln \left( \sum_{j=1}^{nc} \theta_j \tau_{ij} \right) - \sum_{j=1}^{nc} \frac{\theta_j \tau_{ij}}{\sum_{k=1}^{nc} \theta_k \tau_{kj}} \right\}$$

where

$$I_i = \frac{z}{2} (r_i - q_i) - (r_i - 1); \quad \theta_i = \frac{q_i x_i}{\sum_{j=1}^{nc} q_j x_j}; \quad \varphi_i = \frac{r_i}{\sum_{j=1}^{nc} r_j x_j}$$

$$v_i = \frac{q_i \sum_{j=1}^{nc} r_j x_j}{r_i \sum_{j=1}^{nc} q_j x_j}; \quad \tau_{ij} = \exp \left( -\frac{u_{ij}}{RT} \right)$$

<sup>a</sup> Binary interaction parameters are obtained from DECHEMA.

to obtain a good agreement between the experimental and model results.

**RE Model**

Here, it is assumed that the esterification reaction takes place between adsorbed butanol and acetic acid species on the catalyst surface to give unadsorbed butyl acetate and adsorbed water molecules. The rate expression for the RE model can be given by eq 5, where  $K_f$

$$r_i = n \frac{dx_i}{dt} = v_f M_{cat} K_f K_{s,AcH} K_{s,BuOH} \frac{\left( a_{AcH} a_{BuOH} - \frac{1}{K_a} a_{BuAc} a_{H_2O} \right)}{\left( 1 + a'_{AcH} + a'_{BuOH} + a'_{H_2O} \right)^2} \quad (5)$$

and  $K_b$  are the rate constants for the forward and backward reactions, respectively. Also,

$$K_a = \prod a_i^{\nu_i} = \frac{K_f K_{s,AcH} K_{s,BuOH}}{K_b K_{s,H_2O}} \quad (6)$$

and  $a_i = K_{s,i} a_i$ . As can be seen, this model has a total of seven parameters: three adsorption constants, the preexponential factors  $K_f^0$  and  $K_a^0$ , and the energies of activation  $E_f$  and  $E_a$ . If one adopts the equilibrium

constant from Janowsky et al.,<sup>13</sup> still five parameters have to be obtained through regression analysis.

**LHHW Model**

In this model, all of the components were assumed in their adsorbed phases. The rate of reaction for the LHHW model (eq 7) can be written as follows:

$$r_i = n \frac{dx_i}{dt} = v_f M_{cat} K_f K_{s,AcH} K_{s,BuOH} \frac{\left( a_{AcH} a_{BuOH} - \frac{1}{K_a} a_{BuAc} a_{H_2O} \right)}{\left( 1 + a'_{AcH} + a'_{BuOH} + a'_{BuAc} + a'_{H_2O} \right)^2} \quad (7)$$

where

$$K_a = \prod a_i^{\nu_i} = \frac{K_f K_{s,AcH} K_{s,BuOH}}{K_b K_{s,BuAc} K_{s,H_2O}}$$

A total of six parameters, four adsorption constants, the preexponential factor  $K_f^0$ , and the energy of activation  $E_f$ , were determined based on the experimental data using the aforementioned parameter identification method.

**ML Model**

To account for the distribution of water in the resin phase, an empirical constant ( $\alpha$ ) can be introduced in the LHHW model to give an expression for the ML model (eq 8).<sup>21,22</sup> Assuming  $\alpha = 2$  (ML), which was then

$$r_i = n \frac{dx_i}{dt} = v_f M_{cat} K_f K_{s,AcH} K_{s,BuOH} \frac{\left( a_{AcH} a_{BuOH} - \frac{1}{K_a} a_{BuAc} a_{H_2O}^\alpha \right)}{\left( 1 + a'_{AcH} + a'_{BuOH} + a'_{BuAc} + K_{H_2O} a_{H_2O}^\alpha \right)^2} \quad (8)$$

found to be satisfactory, and taking into account the equilibrium constant from Janowsky et al.,<sup>13</sup> still six parameters are required to be determined. The regression analysis was also performed with  $\alpha$  as a model parameter (MLC).

The results obtained from the parameter identification for all of the above models are shown in Table 3. Figures 4–6 show the comparison between experimental data and model predictions for the effect of temperature, catalyst loading, and mole ratio, respectively. Here, it should be noted that the figures show those experimental data which were never used to obtain the intrinsic kinetic parameters by parameter identification. As can be seen from the figures, the agreement between model predictions and experimental data is reasonably well for all of the models. Among all of the models, the ML model (with  $\alpha = 2$ ) is the best model that gives the least residual error. If  $\alpha$  is set as a model parameter, its value, 1.48, after regression gives slightly better results on data fitting. All in all, out of all of the models

**Table 3. Parameters for Different Kinetic Models Used To Fit the Experimental Data**

model	$K_f^0 \times 10^{-6}$ kmol/kg·s	$E_f \times 10^{-3}$ kJ/kmol	$K_a^0$	$E_a \times 10^{-3}$ kJ/kmol	$K_{s,AcH}$	$K_{s,BuOH}$	$K_{s,BuAc}$	$K_{s,H_2O}$	$\alpha$	$\phi \times 10^3$
PH	3.3856	70.660	3.3405	-3.5817						2.5
RE	20.1315	73.4105	3.8207	-3.5817	7.0960	5.0599		8.8146		1.9
ML	14.0093	72.896	3.8207	-3.5817	4.4521	6.9211	3.5995	9.0304	2.00	1.8
MLC	16.9897	73.422	3.8207	-3.5817	4.3756	4.8424	$1 \times 10^{-11}$	8.0663	1.48	1.8

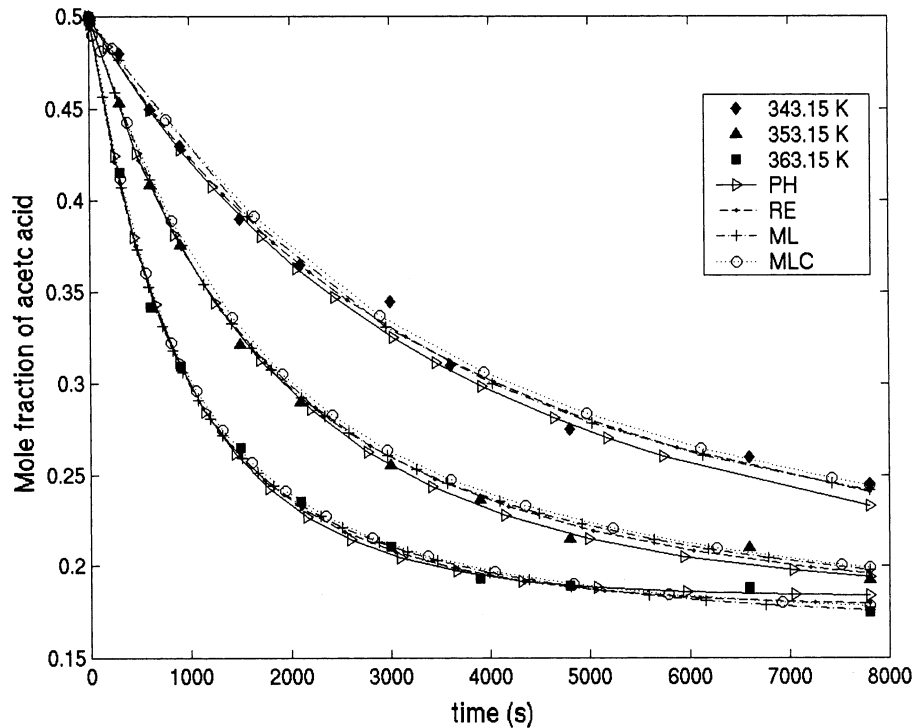


**Figure 4.** Comparison of the effect of temperature on the acetic acid mole fraction.  $M_{cat} = 6.67$  g of catalyst/gmol of AcH and mole ratio of AcH:BuOH = 1:1.

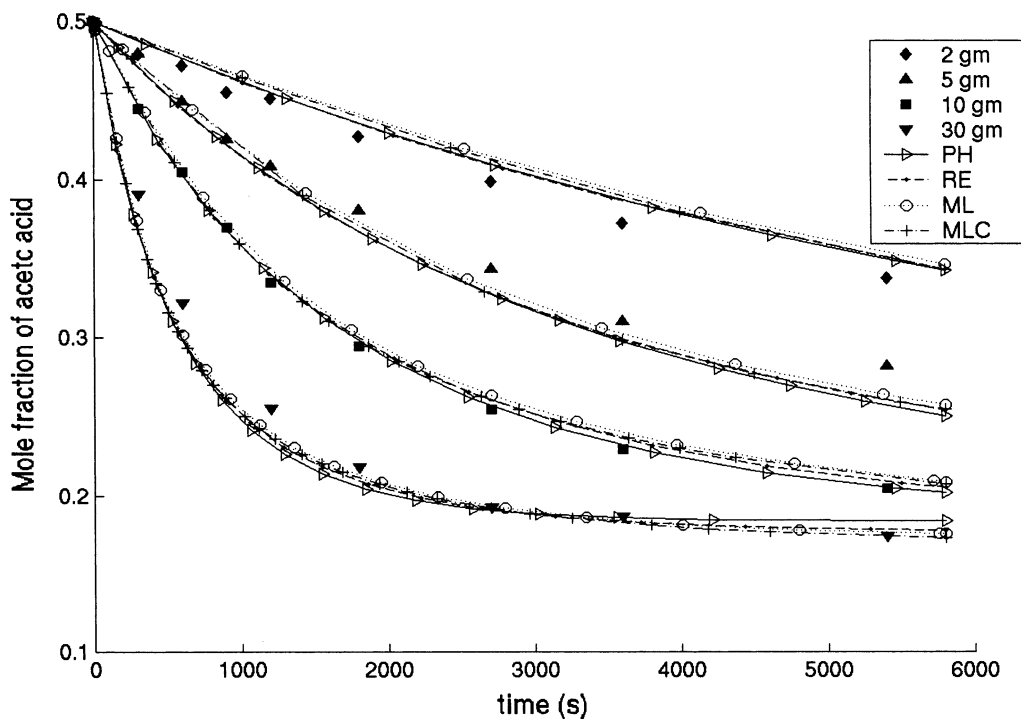


**Figure 5.** Comparison of the effect of catalyst loading on the acetic acid mole fraction.  $T = 356$  K and mole ratio of AcH:BuOH = 1:1. The values in the legend refer to the absolute catalyst weight used for 90 g of acetic acid.

studied, the residual errors involved in RE, ML with  $\alpha = 2$ , and ML with  $\alpha = 1.48$  models are close to each other, and for all practical purposes, these models predict reasonably accurate results on the reaction kinetics studied under the given conditions. It should be noted here that the LHHW model without modification (i.e., with  $\alpha = 1$ ) gives negative values of the adsorption coefficients, indicating that the model is not suitable for this reacting system.

### Side Reaction

As discussed earlier, DBE forms through dehydration of butanol at relatively higher temperature and higher catalyst loading in the presence of dry catalyst. It is very likely, therefore, to obtain DBE in the catalytic stripping section of a reactive distillation column, where all of these conditions prevail. Therefore, knowledge of the kinetic expression for this reaction is also required. Kinetic data were obtained for the tempera-

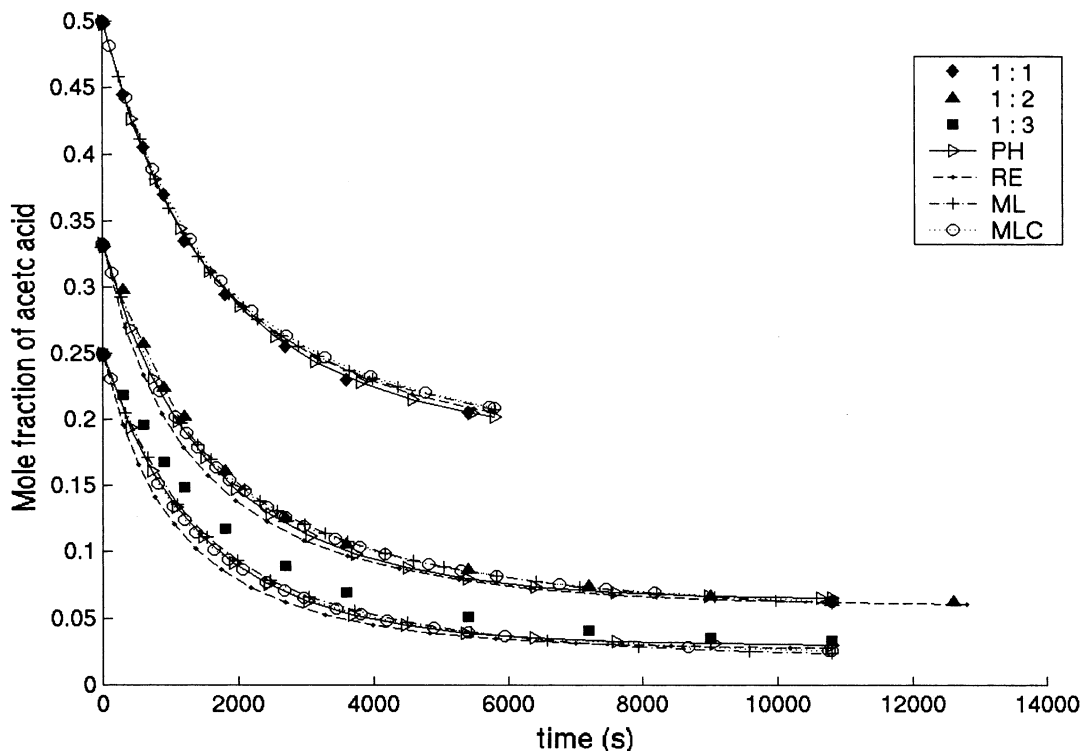


**Figure 6.** Comparison of the effect of mole ratio (ACh:BuOH) on the acetic acid mole fraction.  $T = 356$  K and  $M_{\text{cat}} = 6.67$  g of catalyst/gmol of ACh.

**Table 4. Kinetic Model Parameters for Etherification**

model	$K_{\text{DBE}}^0$ (kmol/kg·s)	$E_{\text{DBE}} \times 10^{-3}$ kJ/kmol	$K_{\text{s,BuOH}}$	$K_{\text{s,DBE}}$	$K_{\text{s,H}_2\text{O}}$	$\alpha$	$\phi \times 10^5$
RE	369.048	68.7961	5.0599		8.81445		9.8
LHHW	361.888	68.6002	5.0599	3.32814	8.81445		7.7
ML	308.146	68.6209	5.0599	3.7887	8.81445	2	8.0

tures between 386 and 399 K and the catalyst loadings over the range 7–17 g of catalyst/gmol of butanol.

Dehydration of butanol to DBE can be considered to be an irreversible reaction because the equilibrium constants for etherification reactions are fairly high.<sup>23</sup> This belief was further strengthened by the results of an experimental run started with a stoichiometric amount of DBE and water in the presence of a catalyst at 403 K, which showed no indication of the presence of *n*-butanol even after 5 h.



Equation 9 can be written for a kinetic expression considering the chemical step as a rate-controlling step.



$$r_i = n \frac{dx_i}{dt} = v_i M_{\text{cat}} K_{\text{DBE}} \frac{(a'_{\text{BuOH}})^2}{(1 + \sum_j a_j)^2} \quad (9)$$

Taking into account the adsorption constant of butanol and water from the main reaction kinetics, only three parameters are required to be obtained, as shown in eq 9: preexponential factor  $K_{\text{DBE}}^0$ , activation energy  $E_{\text{DBE}}$ , and the adsorption constant of DBE. The results of parameter fittings are shown in Table 4. Table 4 also shows the parameter fitting results for the RE model,

where it was assumed that DBE is an unadsorbed molecule, and for the ML model, where an empirical constant ( $\alpha$ ) is introduced for accountability of the distribution of water in the resin phase. Equations 10 and 11 show the kinetic expressions for the RE and ML models, respectively.

$$r_i = n \frac{dx_i}{dt} = v_i M_{\text{cat}} K_{\text{DBE}} \frac{(a'_{\text{BuOH}})^2}{(1 + a'_{\text{BuOH}} + a'_{\text{H}_2\text{O}})^2} \quad (10)$$

$$r_i = n \frac{dx_i}{dt} = v_i M_{\text{cat}} K_{\text{DBE}} \frac{(a'_{\text{BuOH}})^2}{(1 + a'_{\text{BuOH}} + a'_{\text{DBE}} + K_{\text{s,H}_2\text{O}} a_{\text{H}_2\text{O}}^\alpha)^2} \quad (11)$$

For this reaction, the LHHW model gives the best predictions. Figures 7 and 8 show the agreement between experimental results and model predictions for different temperatures and catalyst loadings, respectively.

### Reactions at Boiling Conditions

To validate the obtained kinetics for esterification and etherification reactions, an experiment was performed in a batch reactor at the boiling temperature of the reaction mixture under the conditions of total reflux. The temperature variations during the course of the

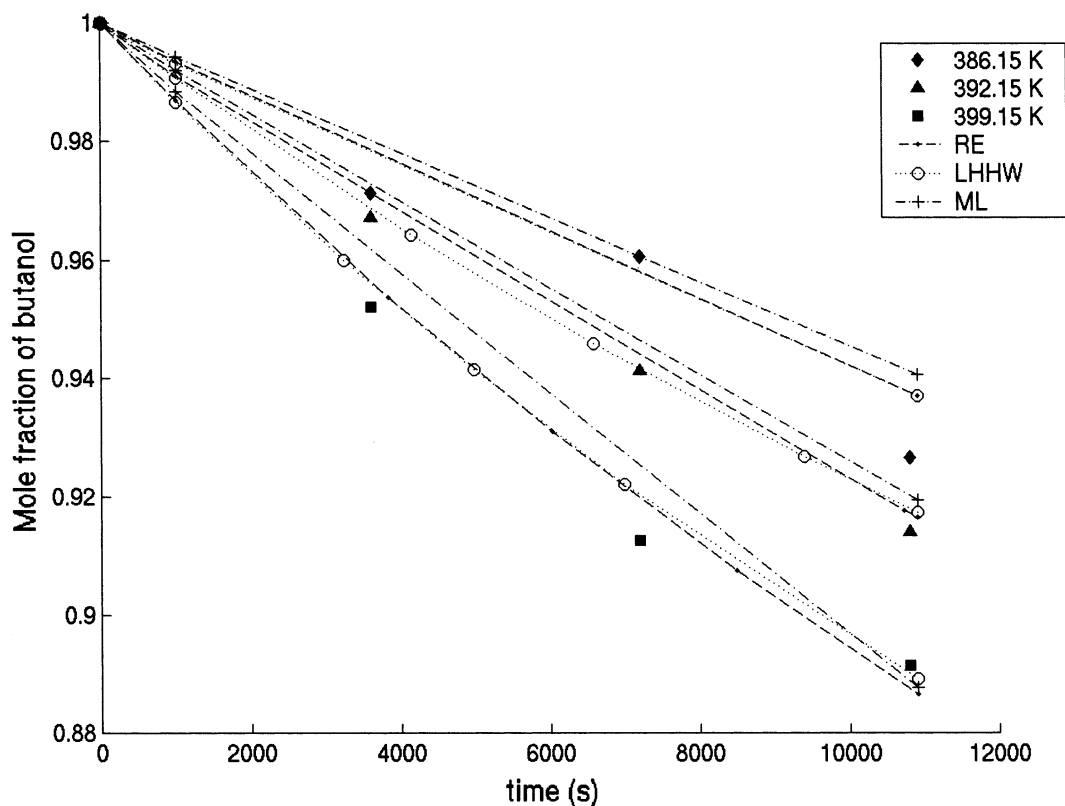


**Figure 7.** Comparison of the different kinetic model effect of temperature.  $M_{\text{cat}} = 26$  g of catalyst/gmol of *n*-BuOH starting with pure BuOH.

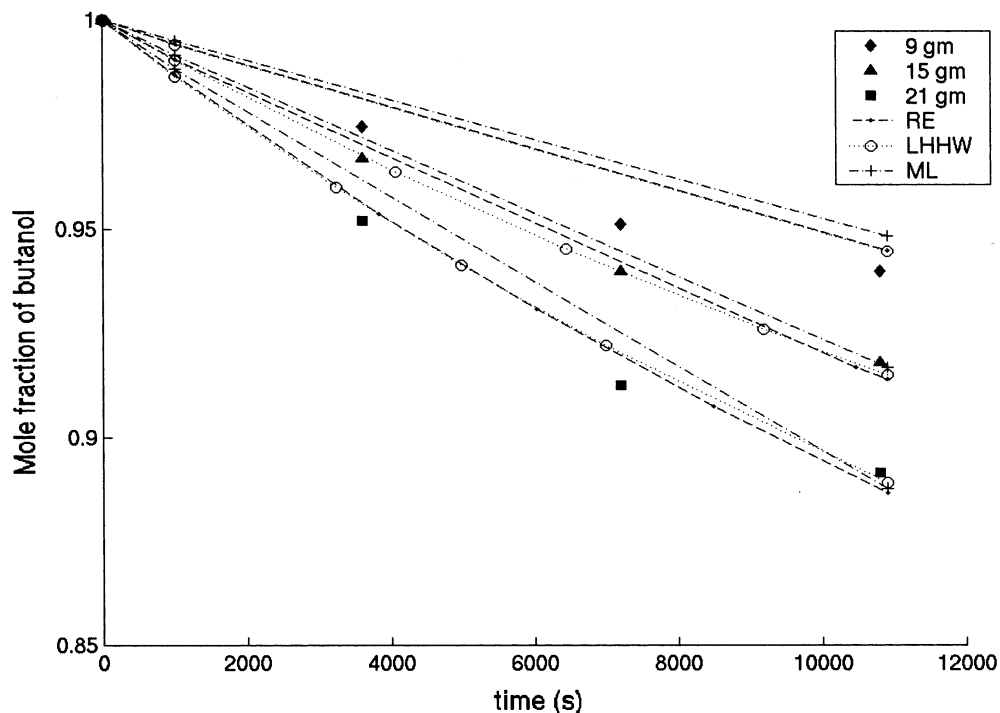


**Figure 8.** Comparison of different kinetic model effect of catalyst loading.  $T = 392$  K. The values in legend refer to the absolute catalyst weight used per 60 g of *n*-BuOH.

reactions were noted. These temperature data along with the kinetics of both reactions can yield computed values of substrate concentrations for the conditions of the experiments. Figure 9 shows a comparison between the experimental and computed acetic acid mole fractions. It can be seen that the kinetic model is in good agreement with the experimental data obtained at

the boiling temperature. Under the temperature, catalyst loading, and mole ratio used for the experimental run, the experimental and kinetic models both show an insignificant amount of DBE formation. This indicates that, even though the kinetic models for etherification and esterification were developed separately, both models compliment each other well.

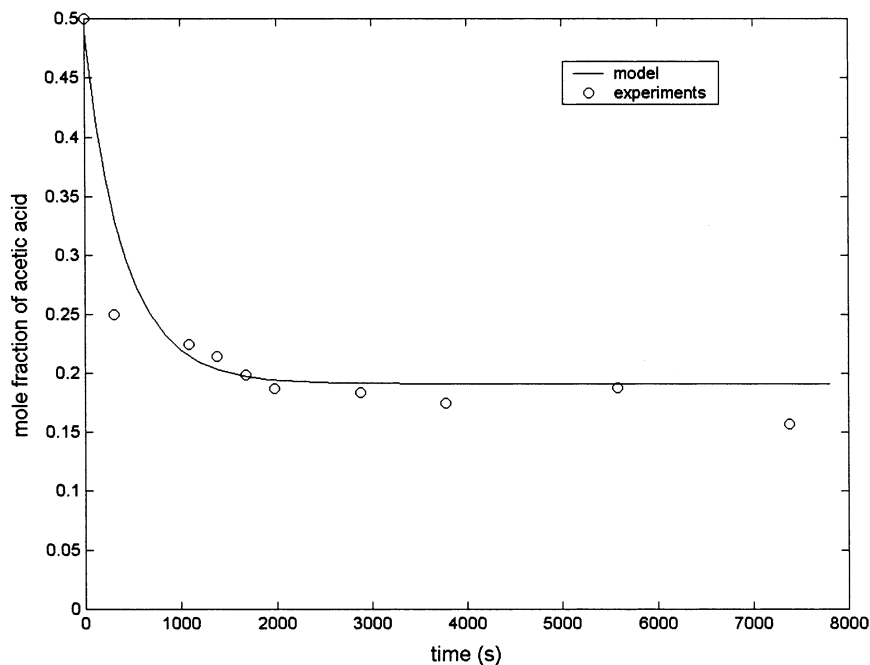


Figure 9. Comparison between calculated and experimental acetic acid mole fractions for reaction at boiling conditions.

## Conclusion

The kinetic data for esterification of butanol with acetic acid and those for etherification of butanol in the presence of ion-exchange resin Amberlyst-15 are generated. The ML and LHHW models explain the data successfully over a wide range of catalyst loadings and temperatures for esterification and etherification reactions, respectively. The independent experiment was performed to generate the reaction data under boiling conditions. The model results with the regressed kinetic parameters are in excellent agreement with the experimental results.

## Nomenclature

$a_i$  = activity of the  $i$ th component in the liquid phase  
 $a'_i$  = product of the adsorption constant and activity for component  $i$   
 $K_a$  = equilibrium constant of esterification  
 $K_a^0$  = preexponential factor for  $K_a$   
 $K_b$  = backward reaction rate constant for esterification, kmol/kg·s  
 $K_{DBE}$  = forward reaction rate constant for etherification, kmol/kg·s  
 $K_{DBE}^0$  = preexponential factor for  $K_{DBE}$ , kmol/kg·s  
 $K_f$  = forward reaction rate constant for esterification, kmol/kg·s  
 $K_f^0$  = preexponential factor for  $K_f$ , kmol/kg·s  
 $K_{s,i}$  = adsorption constant of component  $i$   
 $E_a$  = activation energy for the equilibrium constant of esterification, kJ/kmol  
 $E_{DBE}$  = activation energy for etherification, kJ/kmol  
 $E_f$  = activation energy for the forward rate constant of esterification, kJ/kmol  
 $M_{cat}$  = mass of the catalyst, kg  
 $n$  = molar holdup, kmol  
 $nc$  = number of components  
 $R$  = gas constant, kJ/kmol·K  
 $r_i$  = reaction rate of component  $i$ , kmol/s  
 $T$  = temperature, K  
 $x_i$  = mole fraction of the  $i$ th component in the liquid phase

## Greek Letters

$\alpha$  = constant in modified  $i$ th LHHW model  
 $\gamma_i$  = activity coefficient of component  
 $\nu_i$  = stoichiometric coefficient of  $i$ th component  
 $\phi$  = objective function

## List of Abbreviations

AcH = acetic acid  
 BuAc =  $n$ -butyl acetate  
 BuOH =  $n$ -butanol  
 DBE = di- $n$ -butyl ether  
 LHHW = Langmuir–Hinshelwood–Hougen–Watson model  
 ML = modified LHHW model  
 MLC = variant of the ML model  
 PH = pseudohomogeneous model  
 RE = Eley–Rideal model

## Literature Cited

- (1) Leyes, C. E.; Othmer, D. F. Continuous esterification of butanol and acetic acid, Kinetic and distillation considerations. *Trans. Am. Inst. Chem. Eng.* **1945**, *41*, 157–196.
- (2) Chakrabarty, A.; Sharma, M. M. Cationic exchange resins as catalyst. *React. Polym.* **1993**, *20*, 1–45.
- (3) Zheng, R.; Zeng, J. Catalyst for butyl acetate using strong acidic cation-exchange resin. *Xiamen Daxue Xuebao, Ziran Kexueban* **1997**, *36*, 67–70; *Chem. Abstr.* **127**, 1614845.
- (4) Zheng, R.; Zeng, J. Kinetics of esterification of acetic acid and  $n$ -butanol on strong cation-exchange resin. *Xiamen Daxue*

Xuebao, *Ziran Kexueban* **1998**, 37, 224–227; *Chem. Abstr.* 129, 951425.

(5) Liao, A.; Tong, Z. Synthesis of *n*-butyl acetate catalyzed by Amberlyst. *Huaxue Fanying Gongcheng Yu Gongy* **1995**, 11, 34–45; *Chem. Abstr.* 124, 179409.

(6) Liao, S.; Zhange, X. Study on esterification catalyzed by solid acid catalyst. II Kinetics and mechanism of liquid-phase Esterification. *Hunan Ligong Daxue Xuebao, Ziran Kexueban* **1997**, 25, 88–92; *Chem. Abstr.* 128, 2433638.

(7) Liao, S.; Xu, B.; Li, Z. Catalysis of solid acid catalyst for esterification I preparation and characterization of the catalyst. *Fenzi Cuihua* **1993**, 76, 475–478; *Chem. Abstr.* 120, 1376125.

(8) Li, B.; Li, Z.; Fang, W. Synthesis of *n*-butyl acetate catalyzed by inorganic salts. *Guangxi Huagong* **1998**, 27, 19–22; *Chem. Abstr.* 129, 29335.

(9) Ma, D.; Shuzhen, G. Synthesis of *n*-butyl acetate in liquid phase with zeolites as catalysts. *Shiyon Huagong* **1989**, 18; *Chem. Abstr.* 112, 79882.

(10) Ma, D.; Shuzhen, G.; Ronghin, Y. Continuous synthesis process of *n*-butyl acetate in liquid phase with zeolites as catalysts. *Hauxue Shijie* **1994**, 35, 634–636; *Chem. Abstr.* 123, 173453.

(11) Zheng, H.; Zhung, M.; Li, H. Catalytic property of HZSM5 in the esterification reaction. Effect of cation exchange degree, reaction condition and structure of reactant. *Ranliao Hauxue Xuebao* **1989**, 17, 62–68; *Chem. Abstr.* 112, 178027.

(12) Li, Y.; Lin, G.; Li, Y. Application of zeolites catalyst in the esterification reaction of acetic acid in liquid phase. *Tiayuan Gongue Daxue Xuebao* **1996**, 27, 53–55; *Chem. Abstr.* 126, 225003.

(13) Janowsky, R.; Groebel, M.; Knippenberg, U. *Nonlinear dynamics in reactive distillation—phenomena and their technical use*; Final Report FKZ 03 D 0014 B0; Huels Infracor GmbH: experScience, Marl, 1997.

(14) Venimadhavan, G.; Malone, M. F.; Doherty, M. F. A novel distillate policy for batch reactive distillation with application to production of butyl acetate. *Ind. Eng. Chem. Res.* **1999**, 38, 714–722.

(15) Hanika, J.; Kolena, J.; Smejkal, Q. Butyl acetate via reactive distillation: Modeling and Experiments. *Chem. Eng. Sci.* **1999**, 54, 5205–5209.

(16) Zhicai, Y.; Xianbao, C.; Jing, G. Esterification–distillation of butanol and acetic acid. *Chem. Eng. Sci.* **1998**, 53, 2081–2088.

(17) Saha, B.; Chopade, S. P.; Mahajani, S. M. Recovery of dilute acetic acid through esterification in reactive distillation column. *Catal. Today* **2000**, 60, 147–157.

(18) Minotti, M.; Doherty, M. F.; Malone, M. F. Design for Simultaneous Reaction and Liquid–Liquid Extraction. *Ind. Eng. Chem. Res.* **1998**, 37, 4748–4755.

(19) *NAG Fortran Library Manual*; NAG Ltd.: Oxford, U.K., 1993.

(20) Caracotsios, M.; Stewart, W. Sensitivity analysis of initial value problems with mixed ODEs and algebraic equations. *Comput. Chem. Eng.* **1985**, 9, 359–365.

(21) Lee, M.; Wu, H.; Kang, C.; Lin, H. Kinetics of catalytic esterification of acetic acid and amyl alcohol over Amberlyst 15. *J. Chem. Eng. Jpn.* **2001**, 34, 960–963.

(22) Lee, M.; Wu, H.; Lin, H. Kinetics of catalytic esterification of acetic acid and amyl alcohol over Dowex. *Ind. Eng. Chem. Res.* **2000**, 39, 4094–4099.

(23) Song, W.; Venimadhavan, G.; Manning, J.; Malone, M.; Doherty, M. Measurement of residue curve maps and heterogeneous kinetics in methyl acetate synthesis. *Ind. Eng. Chem. Res.* **1998**, 37, 1917–1928.

*Received for review* July 5, 2002

*Revised manuscript received* January 2, 2003

*Accepted* February 9, 2003

IE0204989